Chen et al. Nanoscale Research Letters 2013, 8:225
http://www.nanoscalereslett.com/content/8/1/225

Nanoscale Research Letters
a SpringerOpen Journal

NANO EXPRESS Open Access

# Enhanced solar energy conversion in Au-doped, single-wall carbon nanotube-Si heterojunction cells

Leifeng Chen[1,2*], Hong He[2,3], Shijun Zhang[1], Chen Xu[1], Jianjiang Zhao[1], Shichao Zhao[2], Yuhong Mi[2] and Deren Yang[1]

## Abstract

The power conversion efficiency (PCE) of single-wall carbon nanotube (SCNT)/n-type crystalline silicon heterojunction photovoltaic devices is significantly improved by Au doping. It is found that the overall PCE was significantly increased to threefold. The efficiency enhancement of photovoltaic devices is mainly the improved electrical conductivity of SCNT by increasing the carrier concentration and the enhancing the absorbance of active layers by Au nanoparticles. The Au doping can lead to an increase of the open circuit voltage through adjusting the Fermi level of SCNT and then enhancing the built-in potential in the SCNT/n-Si junction. This fabrication is easy, cost-effective, and easily scaled up, which demonstrates that such Au-doped SCNT/Si cells possess promising potential in energy harvesting application.

**Keywords:** Solar cell, Single-wall carbon nanotube, Chemical doping, Conductivity, Au nanoparticles, Plasmon resonance

## Background

Photovoltaic devices based on nanomaterials may be one kind of next-generation solar cells due to their potential tendency of high efficiency and low cost [1]. Among them, carbon nanotube (CNT), possessing one-dimensional nanoscale structure, high aspect ratios, large surface area [2], high mobility [3], and excellent optical and electronic properties, could be beneficial to exciton dissociation and charge carrier transport, which allow them to be useful in photovoltaic devices [4-8]. In recent years photovoltaic devices and photovoltaic conversion based on the heterojunctions of CNT and n-type silicon have been investigated [9-12]. In those devices, electron–hole pairs are generated in CNT under illumination and are separated at the heterojunctions. This means that the CNT acts as the active layer of the cells for exciton generation, charge collection, and transportation, while the heterojunction acts for charge dissociation. The conductivity and transparency of the single-wall carbon nanotube (SCNT) films are two important factors for fabricating the higher performance of SCNT/n-Si solar cell. Kozawa had found that the power conversion efficiency (PCE) strongly depended on the thickness of the SCNT network and showed a maximum value at the optimized thickness [13]. Li had found that photovoltaic conversion of SCNT/n-silicon heterojunctions could be greatly enhanced by improving the conductivity of SCNT [14]. Therefore, the efficiency of the solar cells for SCNT/n-Si is directly related to the property of SCNT film. Recently, doping in CNT has been employed to improve the performance of their cells [15-17]. Saini et al. also reported that the heterojunction of boron-doped CNT and n-type Si exhibited the improved property due to boron doping [18]. Bai et al. found that the efficiency of Si-SCNT solar cells is improved to 10% by $H_2O_2$ doping [19]. Furthermore, it was reported that higher performance SCNT-Si hybrid solar cells could be achieved by acid doping of the porous SCNT network [20]. It is believed that the doping of CNT and the reduced resistivity are in favor of the charge collection and prevention of carriers from

* Correspondence: chlf@hdu.edu.cn
[1]State Key Lab of Silicon Materials and Department of Materials Science and Engineering, Zhejiang University, Hangzhou 310027, People's Republic of China
[2]College of Materials and Environmental Engineering, Hangzhou Dianzi University, Hangzhou 310018, People's Republic of China
Full list of author information is available at the end of the article

recombination, so the PCE of the CNT-based solar cells can be enhanced.

In this paper, we prepared a SCNT film on a n-Si substrate by an electrophoretic method, and then doping the SCNT by a simple method in a $HAuCl_4{\cdot}3H_2O$ solution at room temperature [21,22], to improve the PCE as the result of improved conductivity and increased density of carriers. In this experiment, it was found that p-type doping due to Au could shift down the Fermi level and enhanced the work function of SCNT so that the open circuit voltage was increased. It was also found that the conversion efficiency of the Au-doped SCNT cells was significantly increased compared with that of pristine SCNT/n-Si cells.

## Methods

SCNT of 95% purity with an outer diameter of 1 to 2 nm and lengths of 1 to 3 μm were purchased from Chengdu Organic Chemicals Co. Ltd., Chinese Academy of Sciences, (Chengdu, Sichuan, China). In the experiments, 1 to 3 mg of SCNT were added into 50 ml of analytically pure isopropyl alcohol in which $Mg(NO_3)_2{\cdot}6H_2O$ at a concentration of $1 \times 10^{-4}$ M was dissolved. This solution was subjected to the high-power tip sonication for 2 h. A small part of the solution was diluted in 200 ml of isopropyl alcohol and then placed in a sonic bath for about 5 h to form SCNT electrophoresis suspension.

Constructing the homogeneous semitransparent SCNT network is the first step for fabricating SCNT/n-Si photovoltaic conversion cell. So SCNT film was prepared by the method of electrophoretic deposition (EDP) [23]. A piece of n-type silicon wafer (cathode) and a stainless-steel plate (an anode) were immersed into the SCNT electrophoresis suspension at room temperature. The two electrodes were kept in parallel with a gap of 1 cm. The deposition was carried out for 10 min by applying a constant DC voltage of 100 V. After the EDP and drying in air, the SCNT film on the Si wafer was put into a diluted nitric acid solution to remove possible surviving $Mg(OH)_2$ on the surface.

The doping was carried out by means of dipping the SCNT film in a 0.3 mM hydrogen tetrachloroaurate(III) trihydrate ($HAuCl_4{\cdot}3H_2O$) solution at different times. After drying in nitrogen atmosphere, the SCNT film was slowly dipped into deionized water. The SCNT film was peeled from the Si substrate and floated on the water surface. And then the n-type-patterned Si wafer with the thickness of 250 μm and the resistivity of 1 to 10 Ω·cm, which was pre-deposited with a square $SiO_2$ layer of about 300 nm thickness, was immersed into the water to pick up the expanded SCNT films. Finally, the carbon paste was deposited on the SCNT films to form the upper electrode, and a layer of Au with the thickness of approximately 10 nm was deposited on the back side of the patterned Si wafer as the back electrode. The whole process of the heterojunction solar cells of SCNT and Si substrate is illustrated in Figure 1.

The morphology of SCNT network before and after doping was characterized by field emission scanning electronic microscope (FESEM) and transmission electronic microscope (TEM). The Raman spectra were measured with a laser Raman spectrophotometer. The excitation wavelength of the Ar ion laser was 514.5 nm. An ultraviolet–visible spectrometer (Varian Cary 100; Varian Inc., Palo Alto, CA, USA) was used to study the absorption of the SCNT film. The resistance of SCNT film was measured by a four-point probe method. The carrier density and mobility for the pristine SCNT film and doping film were measured with a Hall effect measurement system (Bio-Rad Corp. Hercules, CA, USA). An Oerlikon external quantum efficiency (EQE) measurement system (Oerlikon Co., Pfaffikon, Switzerland) was used to obtain the EQE of solar cells. The characteristics of cell performance were measured under the standard conditions (1 sun, AM 1.5 Global spectrum), using a Berger Flasher PSS 10 solar

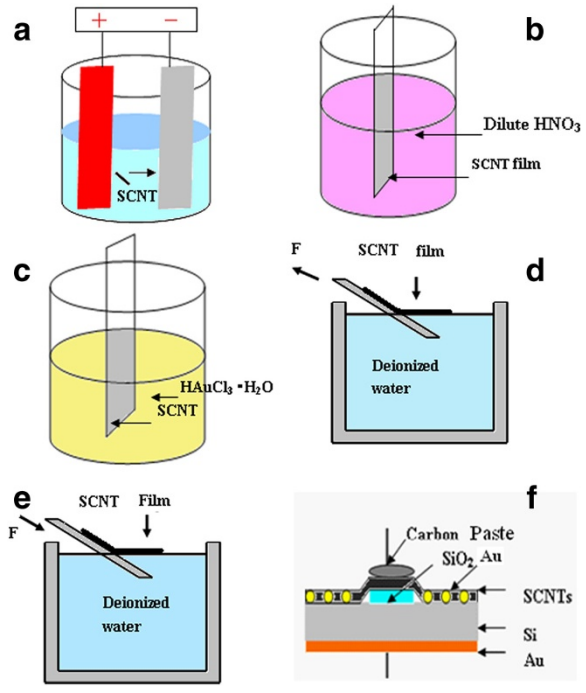


**Figure 1 Schematic diagrams of the EDP, doping and the configuration of a SCNT-on-silicon heterojunction solar cell.** (**a**) EDP SCNT film. (**b**) Removing $Mg(OH)_2$ or $Mg^+$ covered on the SCNT film in dilute nitric acid solution. (**c**) Doping the SCNT film in $HAuCl_3{\cdot}H_2O$ solution. (**d**) A Si substrate covered with SCNTs was slowly dipped into deionized water, and a SCNT film was peeled from the Si substrate and floated on water surface. (**e**) A patterned silicon wafer with a square $SiO_2$ layer was used to pick up the SCNT film. (**f**) The configuration of a SCNT-on-silicon heterojunction solar cell.

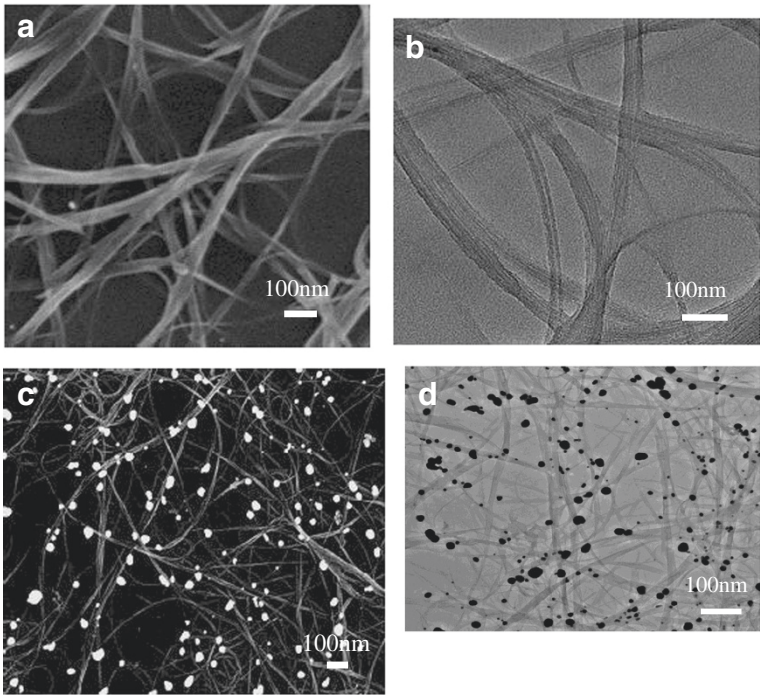


**Figure 2 SEM and TEM images of SCNT networks.** SEM (**a**, **c**) and TEM (**b**, **d**) images of SCNT networks fabricated by EDP and then Au doping.

simulator (Berger Lichttechnik GmbH & Co. KG, Pullach im Isartal, Germany).

## Results and discussion

From Figure 2a, it can be seen the porous network of SCNT were randomly distributed on the Si substrate. The networks of SCNT form the agglomerates of nanotube bundles containing many well-aligned tubes alternating with empty regions. In the Figure 2a, the TEM image shows that the SCNT film before doping is virtually free of catalyst residue. The SCNT film with thicknesses of 20–50 nm shows a transmission of more than 70% in the visible light region. Moreover, the SCNT lying on a substrate form numerous heterojunctions by contacting with the underlying n-Si. Such the semitransparent networks of SCNT ensure the solar light to arrive at interface of SCNT and the underlying Si wafer. After doping, Au nanoparticles with a size in the range of 20–80 nm cover on the surface of the SCNT, as seen in FESEM and TEM (inset) images in Figure 2c and Figure 2d.

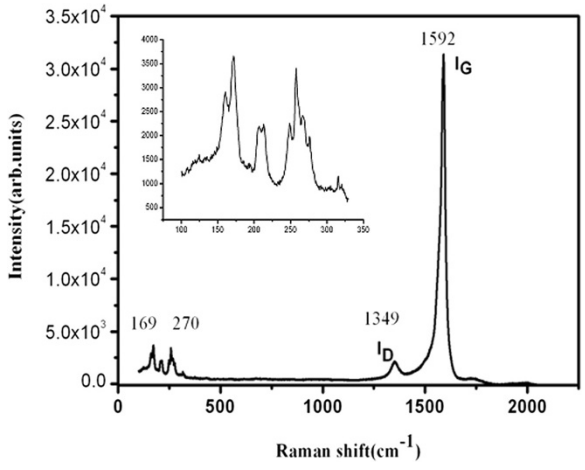


**Figure 3 Raman spectra of the raw SCNT.**

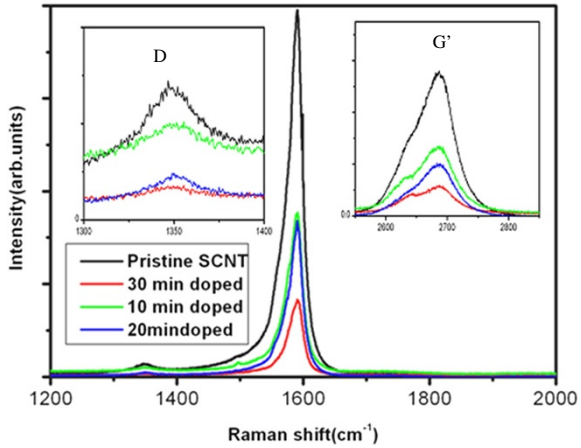


**Figure 4 Raman spectra of pristine and different doping time of SCNT.** The insets are the enlarged images of D and G′ band.

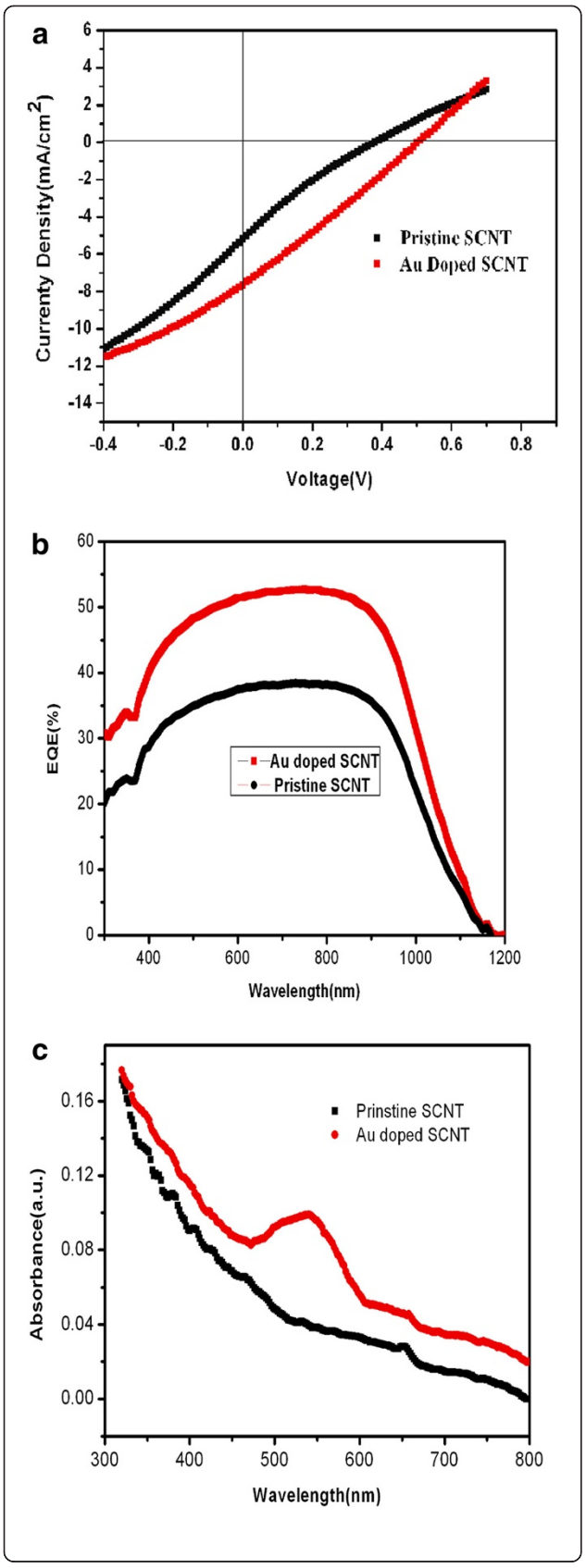


**Figure 5 Current–voltage characteristics, EQE of the solar cell, and optical absorption spectra of SCNT.** (**a**) Current–voltage characteristics of a typical SCNT/n-Si and Au-doped SCNT/n-Si heterojunction device. (**b**) The external quantum efficiency (EQE) of the solar cell obtained before (black line) and after (red line) Au doping. (**c**) Optical absorption spectra of SCNT before (black line) and after (red line) doping.

Figure 3 shows the Raman spectra of the commercial SCNT. It was obtained at room temperature with the laser wavelength of 514.5 nm. It can be seen from the spectra that the characteristic breath and tangential band of SCNT is at 169 to 270 $cm^{-1}$ (inset) and 1,592 $cm^{-1}$, respectively, while the characteristic peak of amorphous carbon is at 1.349 $cm^{-1}$. In general, the content of *a-C* can be calculated by the following formula [24]

$$(I_D/I_G)_{\text{Commercial SWCNTs}} = M_{a\text{-}C} \times (I_D/I_G)_{a\text{-}C} + M_{\text{PureSCNTs}} \times (I_D/I_G)_{\text{PureSCNTs}} \quad (1)$$

In formula (1), $M$ means the molar ratio of the *a-C* and the SCNT, and $M_{a\text{-}C}$ + $M_{\text{pureSWCNTs}}$ =1, $I_D/I_G$ are the ratios of the intensities of D band and G band.

The $I_D/I_G$ value of commercial SCNT calculated from the Raman spectrum as shown in Figure 3 is about 0.70. Usually, the pure SCNT has very small $I_D/I_G$ value and could be assumed as 0.01 [24-26]. Meanwhile, the value of $I_D/I_G$ for *a-C* is similar to that of multiwall CNT (MCNT) and about 1.176 [24]. Thus, the calculated concentration ratio of amorphous carbon and SCNT is about 5.26%. It is obvious that the commercial SCNT is highly pure with little amorphous carbon.

In order to further investigate the effect of Au doping on the properties of SCNT, the Raman spectra for different Au doping samples are shown in Figure 4. In Figure 4, the G bands were up-shift after doping. These changes were consistent with the previous report of the phonon stiffening effect by p-type doping [27,28]. The decreased intensities of the G′ bands manifested the reduction of metallicity of SCNT [29]. The $I_D/I_G$ values of SCNT for different doping time calculated from the Raman spectrum as shown in Figure 3 are almost about of 0.70, although the intensities of $I_D$ and $I_G$ were decreased. These results confirm that the integrity and tubular nature of SCNTs are well preserved during Au doping because of the only process of electrons transferring from SCNT to $Au^{3+}$. This process cannot bring any defects for SCNT [30,31].

Figure 5a shows the current–voltage (*I-V*) curves of the solar cells before and after Au doping. Before doping, the cell exhibits an open circuit voltage ($V_{OC}$) of 0.38 V, a $J_{SC}$ of 5.20 mA/$cm^2$, a fill factor (FF) of 0.18,

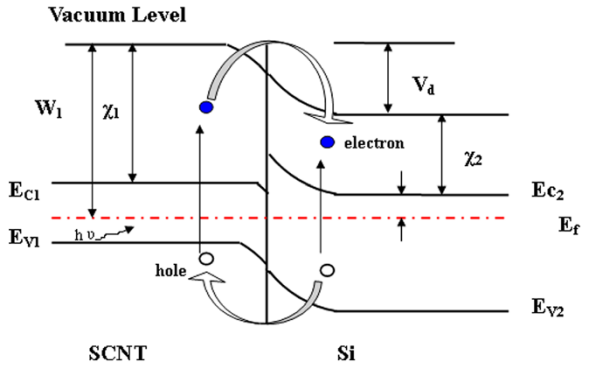


**Figure 6 Energy band diagram of the SCNT/n-Si heterojunction solar cell.** Dashed-dotted red line, hv; blue circle, electron.

and a PCE of 0.36%. After doping, the device shows $V_{OC}$ of 0.50V, $J_{SC}$ of 7.65 mA/cm$^2$, FF of 0.30, and PCE of 1.15%. Both the $J_{SC}$ and $V_{OC}$ were enhanced after Au doping. The PCE was significantly increased to threefold. EQE results shown in Figure 5b indicate that after doping, the EQE increased in the measured spectral range from 300 to 1,200 nm [13,32-34]. The UV–vis spectrum of the Au nanoparticles (Figure 5c) shows a peak at about 535 nm, indicating the presence of a plasmon absorption band. The enhanced optical absorption was observed due to the increased electric field in the active photoactive layer by excited localized surface plasmons around the Au nanoparticles [35,36]. The EQE of the devices with the Au-doped SCNT is higher in the whole visible spectral range than that of the device with the SCNT. The enhanced EQE might be due to the increase of the conductivity of SCNT and of absorption by localized surface plasmons resonance.

In order to compare the SCNT network resistance before and after Au doping, we prepared the SCNT film (1 × 1 cm$^2$) with parallel silver contacts on glass substrate. Four-probe measurements for the SCNT film showed that the sheet resistance can be reduced from 370 to 210 Ω/sq after Au doping. It is known that a standard oxidative purification process can induce p-type charge-transfer doping of SCNT which was observed in their field effect transistors [37]. In our experiments, the SEM and TEM images (the inset of Figure 2b) showed that Au nanoparticles formed during the electroless reduction of Au ions ($Au^{+3}$) on the SCNT film. During the formation of Au nanoparticles on the SCNT surface, $Au^{+3}$ played in the role of electron acceptors and received electrons from SCNT. The formation of Au particles on SCNT can be understood from an electrochemical perspective since the reduction potential of $AuCl_4^-$ ion is higher than the reduction potential of SCNT [38,39]. In aqueous solutions, the following reaction takes place on SCNT:

$$AuCl_4^- + 3e \rightarrow Au^0 \downarrow + 4Cl^- \quad (2)$$

As the electrons are depleted from the SCNT film, the hole carrier density increases, leading to the effective p-type doping effect [40-43]. Au doping can shift down the Femi level and enhance the work function of SCNT [44]; therefore, the built-in potential between SCNT and Si junction can be enhanced. As shown in Figure 6, the built-in voltage can be estimated by [20]

$$V_d \approx (W_1 - \chi_2 - E_{C2} + E_f)/q \quad (3)$$

where $W_1$ is the work function of SCNT, $\chi_2$ is the electron affinity of Si, ($E_{c2}$ – $E_f$) is the energy difference of conduction band and Femi level of n-type Si. Under illumination, the electrons and holes are generated in the SCNT film and the Si substrate. They are collected by the built-in voltage $V_d$ at the junction, where holes and electrons are directed to the SCNT film and the n-Si substrate, respectively. Thus, the formation of the charge accumulation layer on both the sides can reduce the built-in potential, and the reduced potential is equal to the $V_{OC}$. Thereby, the $V_{OC}$ depends on the built-in potential height of the junction $V_d$. Thus, the higher built-in potential height generates the higher $V_{OC}$ under illumination, which can increase the power conversion efficiency of the cell.

In order to better understand the effect of Au doping on the carrier density and mobility of the SCNT, Hall effect measurements were performed for the SCNT film deposited on a glass substrate at room temperature. The Hall effect measurements revealed that the SCNT networks were all p-types conductivity before and after Au doping. After doping, an average carrier density for the

**Table 1 Photovoltaic characteristics of SCNTs-Si solar cell for SCNT immersion in Au solution at different times**

| Time (min) | $J_{SC}$ (mA/cm$^2$) | $V_{oc}$ (V) | FF (%) | PCE (%) | Rs (Ω cm$^2$) | Carrier density (cm$^{-2}$) |
|---|---|---|---|---|---|---|
| 0 | 5.2 ± 0.05 | 0.38 ± 0.02 | 18 ± 0.01 | 0.36 ± 0.06 | 8.72 ± 0.01 | $5.3 \times 10^{18}$ |
| 10 | 7.2 ± 0.04 | 0.45 ± 0.01 | 26 ± 0.01 | 0.84 ± 0.04 | 7.5 ± 0.02 | $7.9 \times 10^{19}$ |
| 20 | 7.65 ± 0.06 | 0.50 ± 0.02 | 30 ± 0.02 | 1.15 ± 0.05 | 5.84 ± 0.01 | $1.4 \times 10^{20}$ |
| 30 | 7.46 ± 0.05 | 0.47 ± 0.01 | 31 ± 0.01 | 1.09 ± 0.04 | 5.65 ± 0.02 | $1.3 \times 10^{21}$ |
| 40 | 7.1 ± 0.02 | 0.46 ± 0.02 | 30 ± 0.01 | 0.98 ± 0.01 | 5.63 ± 0.02 | $1.5 \times 10^{21}$ |

SCNT film increased from $5.3 \times 10^{18}$ to $1.4 \times 10^{20}$ $cm^{-3}$. This enhanced carrier density is advantageous for SCNT/n-Si photovoltaic devices because p doping and the reduced resistivity are in favor of charge collection and preventing carriers from recombination. The gold-hybridization SCNT can provide more charge transport paths, resulting in improved cell PCE more than three folds. Recent studies showed that doping also decreased the tunneling barrier between SCNT and concluded that this is the major fact in the overall film resistance [45-47]. So the devices series resistance (Rs) dropped from 218 Ω (or 8.72 Ω·$cm^2$) in the SCNT/Si cell to 146 Ω (or 5.84 Ω·$cm^2$) in the gold-hybridization SCNT-Si cell.

The effect of the immersion time of SCNT in $HAuCl_4 \cdot H_2O$ solution on the photovoltaic characteristics of the device was investigated. The relative data are shown in the Table 1. It can be seen that with increasing immersion time, the PCE increases. But if the immersion time is too long, the efficiency of the device decreases, although the increasing absorbs of light increases (Figure 5b). Larger particles along with larger surface coverage lead to increased parasitic absorption and reflection, reducing the desired optical absorption in SCNT film layer [48]. In addition, the particles embedded between SCNT and Si substrate will reduce the density of p-n junction and lead to a significantly decrease shunt resistance; therefore, the $J_{SC}$ and $P_{CE}$ decrease. This means that too many Au nanoparticles and very large particles covering on the SCNT will reduce their device PCE.

## Conclusions

In summary, the photovoltaic performance of SCNT-Si heterojunction devices can be significantly improved by doping Au nanoparticles on the wall of SCNT. In the experiments, the PCE, open circuit voltage, short-circuit current density, and fill factor of the devices reached to 1.15%, 0.50 V, 7.65 mA/$cm^2$, and 30% from 0.36%, 0.38v, 5.2, and 18%, respectively. The improved conductivity and the enhanced absorbance of active layers by Au nanoparticles are mainly the reasons for the enhancement of the PCE. It is believed that the photovoltaic conversion efficiency can be further improved by optimizing some factors, such as the density of SCNT, the size and shape of Au nanoparticles, and efficient electrode design.

#### Competing interests

The authors declare that they have no competing interests.

#### Authors' contributions

LC carried out the total experiment, participated in the statistical analysis, and drafted the manuscript. HH, SZ, and CX carried out part of the experiments. JZ and YM participated in the guidance of the experiment. SZ and LC conceived of the study and participated in its design and coordination. DY guided the revision of the manuscript. All authors read and approved the final manuscript.

#### Acknowledgments

The authors would like to appreciate the financial supports of 863 project no. (2011AA050517), the Fundamental Research Funds for the Central Universities, and the financial support from Chinese NSF Projects (no. 61106100).

#### Author details

[1]State Key Lab of Silicon Materials and Department of Materials Science and Engineering, Zhejiang University, Hangzhou 310027, People's Republic of China. [2]College of Materials and Environmental Engineering, Hangzhou Dianzi University, Hangzhou 310018, People's Republic of China. [3]Key Laboratory of Eco-Textiles, Ministry of Education, Jiangnan University, Wuxi 214122, Jiangsu, People's Republic of China.

Received: 14 March 2013 Accepted: 26 April 2013
Published: 10 May 2013

#### References

1. Zhu HW, Wei JQ, Wang KL, Wu DH: **Applications of carbon materials in photovoltaic solar cells.** *Sol Energy Mater & Sol Cells* 2009, **93:**1461–1470.
2. Kim DH, Park JG: **Photocurrents in nanotube junctions.** *Phys Rev Lett* 2004, **93:**107401–107404.
3. Fuhrer MS, Kim BM, Dürkop T, Brintlinger T: **High-mobility nanotube transistor memory.** *Nano Lett* 2002, **2:**755–759.
4. Kou HH, Zhang X, Jiang YM, Li JJ, Yu SJ, Zheng ZX, Wang C: **Electrochemical atomic layer deposition of a $CuInSe_2$ thin film on flexible multi-walled carbon nanotubes/polyimide nanocomposite membrane: structural and photoelectrical characterizations.** *Electrochim Acta* 2011, **56:**5575–5581.
5. Zhang LH, Jia Y, Wang SS, Li Z, Ji CY, Wei JQ, Zhu HW: **Carbon nanotube and CdSe nanobelt Schottky junction solar cells.** *Nano Lett* 2010, **10:**3583–3589.
6. Borgne VL, Castrucci P, Gobbo SD, Scarselli M, Crescenzi D M, Mohamedi M, El Khakani MA: **Enhanced photocurrent generation from UV-laser -synthesized-single-wall-carbon-nanotubes/n-silicon hybrid planar devices.** *Appl Phys Lett* 2010, **97:**193105.
7. Ham MH, Paulus GLC, Lee CY, Song C, Zadeh KK, Choi WJ, Han JH, Strano MS: **Evidence for high-efficiency exciton dissociation at polymer/single-walled carbon nanotube interfaces in planar nano-heterojunction photovoltaics.** *ACS Nano* 2010, **4**(10):6251–6259.
8. Park JG, Akhtar MS, Li ZY, Cho DS, Lee WJ, Yang OB: **Application of single walled carbon nanotubes as counter electrode for dye sensitized solar cells.** *Electrochim Acta* 2012, **85:**600–604.
9. Wei JQ, Jia Y, Shu QK, Gu ZY, Wang KL, Zhuang DM, Zhang G, Wang ZC, Luo JB, Cao AY, Wu DH: **Double-walled carbon nanotube solar cells.** *Nano Lett* 2007, **7**(8):2317–2321.
10. Chen LF, Zhang SJ, Chang LT, Zeng LS, Yu XG, Zhao JJ, Zhao SC, Xu C: **Photovoltaic conversion enhancement of single wall carbon-Si heterojunction solar cell decorated with Ag nanoparticles.** *Electrochim Acta* 2013, **93:**293–300.
11. Gobbo SD, Castrucci P, Scarselli M, Camilli LM, Crescenzi D, Mariucci L, Valletta A, Minotti A, Fortunato G: **Carbon nanotube semitransparent electrodes for amorphous silicon based photovoltaic devices.** *Appl Phys Lett* 2011, **98:**183113.
12. Ong PL, Euler WB, Levitsky IA: **Hybrid solar cells based on single-walled carbon nanotubes/Si heterojunctions.** *Nanotechnology* 2010, **21:**105203.
13. Kozawa D, Hiraoka K, Miyauchi Y, Mouri S, Matsuda K: **Analysis of the photovoltaic properties of single-walled carbon nanotube/silicon heterojunction solar cells.** *Appl Phys Express* 2012, **5:**042304.
14. Li ZR, Kunets VP, Saini V, Xu Y, Dervishi E, Salamo GJ, Biris AR, Biris AS: **$SOCl_2$ enhanced photovoltaic conversion of single wall carbon nanotube/n-silicon heterojunctions.** *Appl Phys Lett* 2008, **93:**243117.
15. Khatri I, Adhikari S, Aryal HR, Soga T, Jimbo T, Umeno M: **Improving photovoltaic properties by incorporating both single walled carbon nanotubes and functionalized multiwalled carbon nanotubes.** *Appl Phys Lett* 2009, **94:**093509.
16. Li C, Chen YL, Ntim SA, Mitra S: **Fullerene-multiwalled carbon nanotube complexes for bulk heterojunction photovoltaic cells.** *Appl Phys Lett* 2010, **96:**143303-1–143303-3.
17. Li ZR, Kunets VP, Saini V, Xu Y, Dervishi E, Salamo GJ, Biris AR, Biris AS: **Light-harvesting using high density p-type single wall carbon nanotube/n-type silicon heterojunctions.** *ACS Nano* 2009, **3:**1407–1441.

18. Saini V, Li ZR, Bourdo S, Kunets VP, Trigwell S, Couraud A, Rioux JL, Boyer C, Nteziyaremye V, Dervishi E, Biris AR, Salamo GJ, Viswanathan T, Biris AS: **Photovoltaic devices based on high density boron-doped single-walled carbon nanotube/n-Si heterojunctions.** *J Appl Phys* 2011, **109:**014321–014326.
19. Bai X, Wang HG, Wei JQ, Jia Y, Zhu HW, Wang KL, Wu DH: **Carbon nanotube-silicon hybrid solar cells with hydrogen peroxide doping.** *Chem Phys Lett* 2012, **533:**70–73.
20. Jia Y, Cao AY, Bai X, Li Z, Zhang LH, Guo N, Wei JQ, Wang KL: **Achieving high efficiency silicon-carbon nanotube heterojunction solar cells by acid doping.** *Nano Lett* 2011, **11**(5):1901–1905.
21. Yang SB, Kong BS, Kim DW, Baek YK, Jung HT: **Effect of Au doping and defects on the conductivity of single-walled carbon nanotube transparent conducting network films.** *J Phys Chem C* 2010, **114:**9296–9300.
22. Kong BS, Jung DH, Oh SK, Han CS, Jung HT: **Single-walled carbon nanotube gold nanohybrids: application in highly effective transparent and conductive films.** *J Phys Chem C* 2007, **111:**8377–8382.
23. Chen LF, Mi YH, Ni HL, Ji ZG, Xi JH, Pi XD: **Enhanced field emission from carbon nanotubes by electroplating of silver nanoparticles.** *J Vac Sci Technol B* 2011, **29**(4):041003.
24. Qian WZ, Liu T, Wei F, Yuan HY: **Quantitative Raman characterization of the mixed samples of the single and multi-wall carbon nanotubes.** *Carbon* 2003, **41:**1851–1854.
25. Ishpal, Panwar OS, Srivastava AK, Kumar S, Tripathi RK, Kumar M, Singh S: **Effect of substrate bias in amorphous carbon films having embedded nanocrystallites.** *Surf Coat Technol* 2011, **206:**155–164.
26. Chiu S, Turgeon S, Terreaul B, Sarkissian A: **Plasma deposition of amorphous carbon films on copper.** *Thin Sol Film* 2000, **359:**275–282.
27. Rao AM, Eklund PC, Bandow S, Thess A, Smalley RE: **Evidence for charge transfer in doped carbon nanotube bundles from Raman scattering.** *Nature* 1997, **388:**257–259.
28. Lee IH, Kim UJ, Son HB, Yoon SM, Yao F, Yu WJ, Duong DL, Choi JY, Kim JM, Lee EH, Lee YH: **Hygroscopic effects on $AuCl_3$-doped carbon nanotubes.** *J Phys Chem C* 2010, **114:**11618–11622.
29. Kim KK, Park JS, Kim SJ, Geng HZ, An KH, Yang CM, Sato K, Saito R, Lee YH: **Dependence of Raman spectra G band intensity on metallicity of single-wall carbon nanotubes.** *Phys Rev B* 2007, **76:**205426.
30. Pramod P, Soumya CC, Thomas KG: **Gold nanoparticle-functionalized carbon nanotubes for light-induced electron transfer process.** *J Phys Chem Lett* 2011, **2:**775–781.
31. Kim SM, Kim KK, Jo YW, Park MH, Chae SJ, Duong DL, Yang CW, Kong J, Lee YH: **Role of anions in the $AuCl_3$-doping of carbon nanotubes.** *ACS Nano* 2011, **5:**1236–1242.
32. Bian ZF, Zhu J, Cao F, Lu YF, Li HX: ***In situ*** **encapsulation of Au nanoparticles in mesoporous core-shell $TiO_2$ microspheres with enhanced activity and durability.** *Chem Commun* 2009, **25:**3789–3791.
33. Li HX, Bian ZF, Zhu J, Huo YN, Li H, Lu YF: **Mesoporous Au/$TiO_2$ nanocomposites with enhanced photocatalytic activity.** *J Am Chem Soc* 2007, **129:**4538–4539.
34. Borgne VL, Gautier LA, Castrucci P, Gobbo SD, Crescenzi MD, Khakani MAE: **Enhanced UV photo-response of KrF-laser-synthesized single-wall carbon nanotubes/n-silicon hybrid photovoltaic devices.** *Nanotechnology* 2012, **23:**215206.
35. Atwater HH, Polman A: **Plasmonics for improved photovoltaic devices.** *Nat Mater* 2010, **9:**205–213.
36. Hou XM, Wang LX, Zhou F, Wang F: **High-density attachment of gold nanoparticles on functionalized multiwalled carbon nanotubes using ion exchange.** *Carbon* 2009, **47:**1209–1213.
37. Snow ES, Novak JP, Campbell PM, Park D: **Random networks of carbon nanotubes as an electronic material.** *Appl Phys Lett* 2003, **82:**2145.
38. Shan B, K Cho J: **First principles study of work functions of single wall carbon nanotubes.** *Phys Rev Lett* 2005, **94:**236602-1–236602-4.
39. Choi HC, Shim M, Bangsaruntip S, Dai H: **Spontaneous reduction of metal ions on the sidewalls of carbon nanotubes.** *J Am Chem Soc* 2002, **124:**9058–9059.
40. Yang SB, Kong BS, Geng JX, Jung HT: **Enhanced electrical conductivities of transparent double-walled carbon nanotube network films by post-treatment.** *J Phys Chem C* 2009, **113:**13658–13663.
41. Li YA, Tai NH, Chen SK, Tsa TY: **Enhancing the electrical conductivity of carbon-nanotube-based transparent conductive films using functionalized few-walled carbon nanotubes decorated with palladium nanoparticles as fillers.** *ACS Nano* 2011, **5:**6500–6506.
42. Chandra B, Afzali A, Khare N, E-Ashry MM, Tulevski GS: **Stable charge-transfer doping of transparent single-walled carbon nanotube films.** *Chem Mater* 2010, **22:**5179–5183.
43. Zhou W, Vavro J, Nemes NM, Fischer JE, Borondics F, Kamaras K, Tanner DB: **Charge transfer and Fermi level shift in p-doped single-walled carbon nanotubes.** *Phys Rev B* 2005, **71:**2054231–2054237.
44. Kim KK, Bae JJ, Park HK, Kim SM, Geng HZ, Park KA: **Fermi level engineering of single-walled carbon nanotubes by $AuCl_3$ doping.** *J Am Chem Soc* 2008, **130:**12757–12761.
45. Nirmalraj PN, Lyons PE, De S, Coleman JN, Boland JJ: **Electrical connectivity in single-walled carbon nanotube networks.** *Nano Lett* 2009, **9:**3890–3895.
46. Stadermann M, Papadakis SJ, Falvo MR, Novak J, Snow E, Fu Q, Liu J, Fridman Y, Boland JJ, Superfine R, Washburn S: **Nanoscale study of conduction through carbon nanotube networks.** *Phys Rev B* 2004, **69:**201402.
47. He Y, Zhang J, Hou S, Wang Y, Yu Z: **Schottky barrier formation at metal electrodes and semiconducting carbon nanotubes.** *Appl Phys Lett* 2009, **94:**093107.
48. Akimov YA, Koh WS, Ostrikov K: **Enhancement of optical absorption in thin-film solar cells through the excitation of higher-order nanoparticle plasmon modes.** *Opt Express* 2009, **17**(12):1015–1019.

doi:10.1186/1556-276X-8-225
**Cite this article as:** Chen *et al.*: Enhanced solar energy conversion in Au-doped, single-wall carbon nanotube-Si heterojunction cells. *Nanoscale Research Letters* 2013 **8**:225.